

Quartic force field predictions of the fundamental vibrational frequencies and spectroscopic constants of the cations HOCO⁺ and DOCO⁺

Ryan C. Fortenberry, Xinchuan Huang, Joseph S. Francisco, T. Daniel Crawford, and Timothy J. Lee

Citation: *J. Chem. Phys.* **136**, 234309 (2012); doi: 10.1063/1.4729309

View online: <http://dx.doi.org/10.1063/1.4729309>

View Table of Contents: <http://jcp.aip.org/resource/1/JCPSA6/v136/i23>

Published by the [American Institute of Physics](#).

Additional information on *J. Chem. Phys.*

Journal Homepage: <http://jcp.aip.org/>

Journal Information: http://jcp.aip.org/about/about_the_journal

Top downloads: http://jcp.aip.org/features/most_downloaded

Information for Authors: <http://jcp.aip.org/authors>

ADVERTISEMENT



ACCELERATE AMBER AND NAMD BY 5X.
TRY IT ON A FREE, REMOTELY-HOSTED CLUSTER.

LEARN MORE

Quartic force field predictions of the fundamental vibrational frequencies and spectroscopic constants of the cations HOCO⁺ and DOCO⁺

Ryan C. Fortenberry,^{1,a)} Xinchuan Huang,^{2,b)} Joseph S. Francisco,³ T. Daniel Crawford,¹ and Timothy J. Lee^{4,c)}

¹Department of Chemistry, Virginia Tech, Blacksburg, Virginia 24061, USA

²SETI Institute, 189 Bernardo Avenue, Suite 100, Mountain View, California 94043, USA

³Department of Chemistry, Purdue University, West Lafayette, Indiana 47907, USA

⁴NASA Ames Research Center, Moffett Field, California 94035-1000, USA

(Received 20 March 2012; accepted 25 May 2012; published online 20 June 2012)

Only one fundamental vibrational frequency of protonated carbon dioxide (HOCO⁺) has been experimentally observed in the gas phase: the ν_1 O–H stretch. Utilizing quartic force fields defined from CCSD(T)/aug-cc-pVXZ ($X = T, Q, 5$) complete basis set limit extrapolated energies modified to include corrections for core correlation and scalar relativistic effects coupled to vibrational perturbation theory and vibrational configuration interaction computations, we are predicting the full set of gas phase fundamental vibrational frequencies of HOCO⁺. Our prediction of ν_1 is within less than 1 cm⁻¹ of the experimental value. Our computations also include predictions of the gas phase fundamental vibrational frequencies of the deuterated form of the cation, DOCO⁺. Additionally, other spectroscopic constants for both systems are reported as part of this study, and a search for a *cis*-HOCO⁺ minimum found no such stationary point on the potential surface indicating that only the *trans* isomer is stable. © 2012 American Institute of Physics. [<http://dx.doi.org/10.1063/1.4729309>]

I. INTRODUCTION

Computational work on protonated carbon dioxide (HOCO⁺) dates back more than 35 years¹ to when Herbst and co-workers² began to hypothesize about the existence of this cation in the interstellar medium (ISM). CISD/DZP computations¹ gave clues about the rotational constants necessary for its suggested detection in the ISM, which came five years later in 1981.³ The interstellar presence of HOCO⁺ was confirmed in 1984 by further laboratory studies by Bogey and co-workers⁴ which matched the observational data. In the intervening years, HOCO⁺ has been detected or strongly suggested to be present in numerous interstellar sightlines^{5–9} and is also known to be significant in various terrestrial and interstellar chemical processes,^{10–17} as well as a useful intermediate in the study of the OH + CO potential surface.^{18–22} Additionally, only the *trans* conformer of HOCO⁺ has been observed experimentally.²⁰

Initial computation of the HOCO⁺ rotational constants by Green and co-workers¹ was followed by numerous theoretical studies over the next decade designed to provide more accurate and complete spectroscopic data in the rotational and vibrational energy regimes as computer hardware and quantum chemical theory progressed.^{23–26} Ultimately, experiments by Amano and Tanaka^{27,28} in 1985 and further work by Bogey and co-workers²⁹ in 1988 were able to provide conclusive gas phase experimental data clearly reporting the spectroscopic constants and geometrical parameters of HOCO⁺. Additionally, Amano and Tanaka^{27,28} reported the vibrational

frequency of the O–H ν_1 stretch at 3375.374 13 cm⁻¹. Frisch and co-workers²⁶ offered the first theoretically computed harmonic vibrational frequencies earlier in 1985, and their theoretical rotational constants along with those from DeFrees and co-workers²⁴ from 1982 were integral to the conclusive assignment of the 3375.374 13 cm⁻¹ band to HOCO⁺ in Amano and Tanaka's experiments. The other five gas phase fundamental vibrational frequencies of HOCO⁺ have not been reported in the literature.

With the use of HOCO⁺ in the analysis of the OH + CO potential surface²⁰ and the emergence of high-resolution observational data from NASA missions like the Stratospheric Observatory for Infrared Astronomy (SOFIA), the need for an understanding of the fundamental physics and more detailed rovibrational reference data of experimentally extant and rotationally observed interstellar species is also growing. Since HOCO⁺ is a known reactant in OH + CO studies^{20,21} and has been shown to exist in the ISM,³ its infrared signature should be present in spectra taken in either of these environments. However, the necessary reference data for the study of HOCO⁺ in the ISM or laboratory environments are far from complete. Experiment has not progressed beyond elucidation of the ν_1 frequency of HOCO⁺ in the gas phase or even just a few of the fundamentals in matrix isolation studies, and previous theoretical studies have not been robust enough to provide the accuracy necessary for a solid estimation of the full set of fundamental vibrational frequencies.

Francisco³⁰ computed various properties of HOCO⁺ using coupled cluster computations [CCSD(T)/6-311G(3df, 3pd)] and competently reports close correlation between theoretically predicated and experimental rotational constants, for instance. However, the vibrational frequencies reported in this study are harmonic in nature, as a result of the study scope,

a) r410@vt.edu.

b) Xinchuan.Huang-1@nasa.gov.

c) Timothy.J.Lee@nasa.gov.

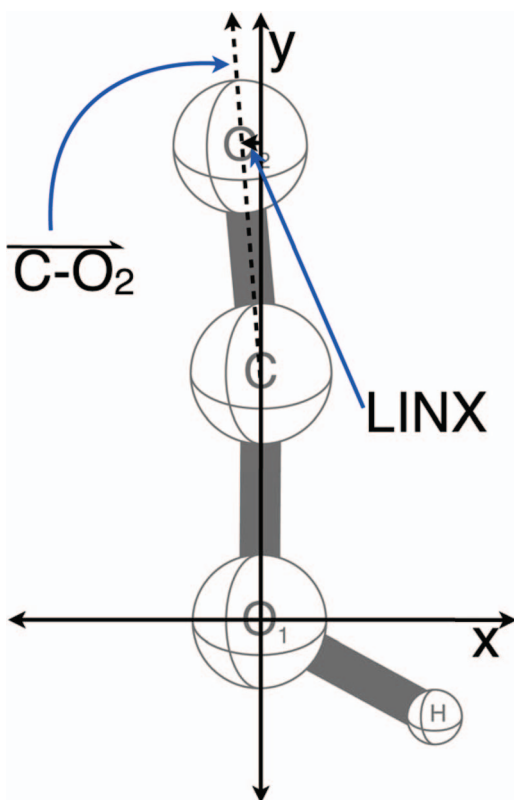


FIG. 1. The HOCO^+ system and a visible representation of the LINX coordinate as discussed in the text.

and cannot provide the necessary accuracy (errors are on the order of 100 cm^{-1} for ν_1) for the fundamental vibrational frequencies for any type of comparison. Jacox and Thompson³¹ report matrix isolation (HOCO^+ in a Ne matrix) fundamental vibrational frequencies for the first two bond stretching frequencies of HOCO^+ and DOCO^+ , ν_1 and ν_2 (the $\text{H}-\text{O}_1$ and $\text{C}-\text{O}_2$ stretches; see Fig. 1), and the ν_4 $\text{H}-\text{O}_1-\text{C}$ bend. A 120 cm^{-1} shift between the HOCO^+ gas phase ν_1 frequency and that observed in the Ne matrix was noted. Hence, the matrix isolation frequencies of the other stretches will differ from their gas phase counterparts, but the nature of these differences cannot be categorically determined. Even so, these condensed phase results provide a very good starting guess as to what the gas phase frequencies may be and may give clues as to how well more accurate theoretical computations perform.

Our previous work on the *trans*- HOCO radical³² and the *cis*- HOCO radical and anion³³ provide good theoretical prediction of gas phase fundamental vibrational frequencies (within 4 cm^{-1} of the experimental fundamentals) and also spectroscopic constants of those systems. The same techniques are being applied to study the HOCO^+ cation and its deuterated counterpart DOCO^+ here. Highly accurate quartic force fields (QFFs) and established rovibrational analysis methods are known to give fundamental vibrational frequencies that are within 5 cm^{-1} or less of the experimental values for various systems.^{32,34-38} In this paper, we will discuss the computational procedure and results for the prediction of the known and unknown fundamental vibrational frequencies and spectroscopic constants of HOCO^+ and DOCO^+ .

II. COMPUTATIONAL DETAILS

Using the same methodology laid forth in our previous studies of the HOCO radicals and anion,^{32,33} coupled cluster theory at the singles, doubles, and perturbative triples [CCSD(T)] (Ref. 39) level is utilized for both the geometry optimization of the HOCO^+ cation as well as for the computation of quartic force fields.^{34,38,40-42} All electronic structure computations are Born-Oppenheimer in nature. Hence, the energies at the points on the potential surface and the resulting force constants will not differ between HOCO^+ and DOCO^+ . As HOCO^+ (and DOCO^+) is a closed-shell cation, all computations undertaken are based on spin-restricted Hartree Fock (RHF) (Refs. 43 and 44) reference wavefunctions. Geometry optimizations of the reference geometry make use of the aug-cc-pV5Z basis set,⁴⁵⁻⁴⁷ while a modification to each bond length and bond angle is included to account for core correlation effects. Computation of the core-correlation effects make use of the Martin and Taylor basis sets⁴⁸ specifically designed to treat core-correlation.

Individual displacements of 0.005 \AA for bond lengths, 0.005 radians for bond angles, and 0.005 unitless displacements of LINX/LINY coordinates, which are required for the necessary pseudo-linear coordinate scheme, generate the 743 symmetry-unique points necessary to define the QFF for this C_s molecule. The definition of the CcCR QFF requires several computations at each point in order to define a composite energy to adequately describe the QFF.^{32,33,36-38} These include CCSD(T)/aug-cc-pVXZ (for $X = \text{T, Q, 5}$) computations where the subsequent energies may be extrapolated out to the complete basis set (CBS) limit by way of a three-point formula.⁵⁰ Even though augmented basis sets are typically not necessary for the computation of properties related to the ground states of cations, the use of these basis sets allows for direct comparison to the corresponding QFFs from our previous studies of HOCO systems. Besides the three energies computed to give the CBS energy, the CcCR QFF also requires computations of scalar relativistic effects⁵¹ with use of the aug-cc-pVTZ-DK basis set and also core-correlation effects which were described in the previous paragraph. The CR QFF lacks the “cC” term in our QFF moniker as it does not make use of core-correlation effects, but it still includes the CBS limit extrapolated energy (the “C” term) and the scalar relativistic correction (the “R” term). All geometry optimizations and energy point computations were performed with the MOLPRO 2010.1 program.⁵²

A tight least squares fit (where the sum of the residuals squared is less than 10^{-16} a.u.²) of the composite energies at each of the points provides the equilibrium geometry and the force constants for a given QFF. The INTDER program⁴⁹ is employed to evaluate the cartesian derivatives from the force constants. Then, the fundamental vibrational frequencies are computed via the SPECTRO program⁵³ for VPT (Refs. 54-56) and via the MULTIMODE program^{57,58} for the VCI method. The variational VCI computations in MULTIMODE require that the simple internal force constants are transformed into Morse-Cosine coordinates⁴² so that the VCI computations give reasonable results. Additionally, SPECTRO is responsible for the prediction of all the spectroscopic constants reported in this work.

III. RESULTS AND DISCUSSION

A. HOCO⁺

The equilibrium structure of the *trans*-HOCO⁺ cation is shown in Fig. 1, and the geometrical parameters and the rotational constants are listed in Table I, while these same parameters for DOCO⁺ are listed in Table II. Furthermore, the CcCR QFF zero-point data are also listed in Table I. The agreement between equilibrium geometries done as part of this study and those optimized by Francisco³⁰ with CCSD(T)/6-311G(3df, 3pd) is very good. We make our theoretical comparisons to data from Ref. 30 since comparison between the CCSD(T)/6-311G(3df, 3pd) results and previous data are given therein.

Similarly, our rotational constants closely match Francisco's, and the harmonic vibrational frequencies reported in both studies are in accordance with one another. Our CcCR QFF zero-point geometry and associated rotational constants are within 2% of their corresponding experimental values, as well.²⁹ Our B_0 and C_0 rotational constants match experiment to within 0.001 cm⁻¹. Differently, the A_0 rotational constant is not quite as close to the experimental observations since the difference between these values is 0.2 cm⁻¹. This larger error in A_0 is probably the result of compounded minor errors in bond lengths along the principle axis, whereas these effects are not as great in the minor axes. The bond distances and bond angles vary by as much as 0.02 Å and 0.7°, respectively.

TABLE I. The minimum energy structure, rotational constants, harmonic vibrational frequencies, vibration-rotation interaction constants, and quartic and sextic centrifugal distortion constants of *trans*-HOCO⁺ computed from the CcCR QFF as compared to experiment and previous theoretical work.

Zero-point			Equilibrium		
	This work	Experiment ^a	This work	Francisco ^b	
R(O ₁ -H)	0.992 09 Å	0.9766 Å	R(O ₁ -H)	0.982 46 Å	0.983 Å
R(C-O ₁)	1.224 80 Å	1.2085 Å	R(C-O ₁)	1.222 46 Å	1.228 Å
R(C-O ₂)	1.123 48 Å	1.1400 Å	R(C-O ₂)	1.121 65 Å	1.126 Å
∠H-O ₁ -C	118.716°	119.38°	∠O ₁ -C-O ₂	118.253°	117.7°
∠O ₁ -C-O ₂	174.446°	174.39°	∠H-O ₁ -C	174.370°	174.3°
A_0	26.176 76 cm ⁻¹	26.349 93 cm ⁻¹	A_e	25.432 44 cm ⁻¹	25.067 3 cm ⁻¹
B_0	0.359 82 cm ⁻¹	0.359 37 cm ⁻¹	B_e	0.360 87 cm ⁻¹	0.358 11 cm ⁻¹
C_0	0.354 37 cm ⁻¹	0.353 89 cm ⁻¹	C_e	0.355 82 cm ⁻¹	0.353 08 cm ⁻¹

Freq (in cm ⁻¹)				
Mode	Description	This work	Previous ^b	
ω_1	a' O ₁ -H stretch	3561.5	3479	
ω_2	a' C-O ₂ stretch	2441.1	2428	
ω_3	a' C-O ₁ stretch	1247.1	1240	
ω_4	a' H-O ₁ -C bend	1066.3	1066	
ω_5	a' O ₁ -C-O ₂ bend	535.6	517	
ω_6	a'' torsional mode	590.0	566	

Vib-rot constants (MHz)				Distortion constants			Watson S reduction					
Mode	α^A	α^B	α^C	(MHz)	(Hz)		(MHz)			(Hz)		
1	39027.9	10.8	17.4	τ'_{aaaa}	-2916.787	Φ_{aaa}	3.418×10^6	Theory	Exp. ^c	Theory		
2	4974.0	79.3	77.9	τ'_{bbbb}	-0.014	Φ_{bbb}	0.000	D_J	3.433×10^{-3}	3.498×10^{-3}	H_J	-0.002
3	5296.2	33.5	32.5	τ'_{cccc}	-0.013	Φ_{ccc}	-0.002	D_{JK}	0.852	0.935 85	H_{JK}	0.885
4	-107082.2	-7.5	6.5	τ'_{aabb}	-2.865	Φ_{aab}	3815.517	D_K	728.341	1123.57 ^d	H_{KJ}	-89.415
5	22024.0	-16.1	-31.3	τ'_{aacc}	0.569	Φ_{abb}	1.965	d_1	-4.148×10^{-5}	-5.217×10^{-5}	H_K	3.418×10^6
6	-8867.4	-37.0	-16.3	τ'_{bbcc}	-0.014	Φ_{aac}	-3904.046	d_2	-9.138×10^{-6}	-1.710×10^{-5}	h_1	0.000
						Φ_{bbc}	0.003				h_2	0.000
						Φ_{acc}	-0.590				h_3	0.000
						Φ_{bcc}	-0.002					
						Φ_{abc}	2.064					

^aSubmillimeter wave spectroscopy from Ref. 29.

^bReference 30.

^cAll given in Ref. 29 except for D_K .

^dThe experimental D_K value is from Ref. 28.

TABLE II. The CcCR minimum energy structure, rotational constants, harmonic vibrational frequencies, vibration-rotation interaction constants, and quartic and sextic centrifugal distortion constants of DOCO^+ .

	Zero-point	Experiment ^a	Equilibrium ^b
R(O ₁ -D)	0.989 85 Å		0.982 46 Å
R(C-O ₁)	1.225 17 Å		1.222 46 Å
R(C-O ₂)	1.123 27 Å		1.121 65 Å
∠D-O ₁ -C	118.557°		118.253°
∠O ₁ -C-O ₂	174.404°		174.370°
A _{0/e}	14.398 20 cm ⁻¹	14.467 12 cm ⁻¹	14.068 86 cm ⁻¹
B _{0/e}	0.339 47 cm ⁻¹	0.339 03 cm ⁻¹	0.340 51 cm ⁻¹
C _{0/e}	0.330 97 cm ⁻¹	0.330 52 cm ⁻¹	0.332 46 cm ⁻¹

Mode	Description	Freq (in cm ⁻¹)
ω ₁	a' O ₁ -D stretch	2603.1
ω ₂	a' C-O ₂ stretch	2443.8
ω ₃	a' C-O ₁ stretch	1230.1
ω ₄	a' D-O ₁ -C bend	861.5
ω ₅	a' O ₁ -C-O ₂ bend	491.5
ω ₆	a'' torsional mode	586.8

Vib-rot constants (MHz)				Distortion constants				Watson <i>S</i> reduction			
Mode	α ^A	α ^B	α ^C	(MHz)		(Hz)		(MHz)		(Hz)	
1	17364.1	12.0	20.1	τ _{aaaa} ^t	-1117.540	Φ _{aaa}	7.680×10 ⁵	Theory	Exp. ^c	Theory	
2	1920.7	71.4	69.1	τ _{bbbb} ^t	-0.013	Φ _{bbb}	0.001	D _J	3.041×10 ⁻³	3.0919×10 ⁻³	H _J 0.000
3	3258.6	34.5	34.3	τ _{cccc} ^t	-0.011	Φ _{ccc}	0.000	D _{JK}	0.332	0.319 89	H _{JK} 0.506
4	-59276.4	-4.1	7.4	τ _{aabb} ^t	-1.529	Φ _{aab}	1889.461	D _K	279.050	338	H _{KJ} -249.891
5	29801.7	-14.2	-28.2	τ _{aaac} ^t	0.177	Φ _{abb}	1.326	d ₁	-1.095×10 ⁻⁴	-1.293×10 ⁻⁴	H _K 7.683×10 ⁵
6	-12815.3	-37.1	-13.4	τ _{bbcc} ^t	-0.014	Φ _{aac}	-2319.570	d ₂	-2.218×10 ⁻⁵	-7.77×10 ⁻⁵	h ₁ 0.000
						Φ _{bbc}	0.000				h ₂ 0.000
						Φ _{acc}	-0.113				h ₃ 0.000
						Φ _{bcc}	-0.000				
						Φ _{abc}	2.083				

^aFrom Ref. 29 which does not report geometric parameters.^bUnder the Born-Oppenheimer approximation, the equilibrium geometry will be the same as HOCO^+ .^cReference 29.

Even so, these deviations are still not very large, and other similarly small differences are predicted in the studies of the HOCO radicals and anion.^{32,33}

Besides the geometrical parameters, the spectroscopic constants for HOCO^+ are also listed in Table I, while the anharmonic constant matrices for both HOCO^+ and DOCO^+ are given in Table III. Table II of Ref. 29 provides centrifugal distortion constants of HOCO^+ . Comparison of this experimental data to our results in Table I shows that the theoretically computed D_J , D_{JK} , d_1 , and d_2 values are in good agreement with their experimental counterparts. However, D_K is 400 MHz less than the 1123.57 MHz reported by Amano and Tanaka,²⁸ but Bogey and co-workers²⁹ discuss the uncertainties affiliated with the experimental measurement of this value due to a low number of observed rotational branches.

Saave and co-workers²⁰ mention that no *cis* conformer of HOCO^+ has been detected. CCSD(T)/aug-cc-pV5Z ge-

ometry optimizations conducted in this study are not able to find a point on the potential surface where *cis*- HOCO^+ exists as a minimum energy structure. Geometry optimizations starting from a *cis* conformation quickly revert to the *trans* arrangement of the atoms. Also, a potential energy scan of bending just the O₁-C-O₂ bond angle from the *trans* conformer at 165° through linear to 110° in the *cis* conformer was undertaken. The resulting plot of bond angle versus energy is simply hyperbolic in nature and does not report any minima besides the known global minimum at about 174° for the *trans* conformer. This result indicates that the *cis* conformer of this cation is not stable, and it offers at least an initial explanation as to why the *cis*- HOCO^+ has not been observed experimentally.

For HOCO^+ , the equilibrium O₁-C-O₂ bond angle is nearly linear at 174.4°, while this angle is between 111° and 131° for the radicals and anion.^{32,33} Hence, it is necessary to use pseudo-linear coordinates, LINX and LINY available in

TABLE III. CcCR QFF anharmonic constant matrix (in cm^{-1}) for HOCO^+ and DOCO^+ .^a

	Mode	1	2	3	4	5	6
HOCO^+	1	-87.943					
	2	-5.652*	-13.110				
	3	-5.069	-14.041*	-3.947*			
	4	-14.094*	2.505*	2.248*	-19.151		
	5	0.321	-10.903	-5.205*	5.718	1.837*	
	6	-1.456	-9.995	-5.482*	3.284	46.038	2.120*
DOCO^+	1	-45.855					
	2	-7.087	-12.760				
	3	-0.377*	-12.892*	-4.870*			
	4	-4.849	-0.436	-1.096*	-8.395		
	5	0.415	-10.780	-5.370*	9.286	1.747*	
	6	-2.621	-7.342	5.433*	-2.028*	19.712	-0.497

^aModes marked with an asterisk (*) are effected by Fermi resonances.

the INTDER program,⁴⁹ for the description of the $\text{O}_1-\text{C}-\text{O}_2$ bond angle as well as the torsional mode for the VPT and VCI computations. The other modes of HOCO^+ may still be described from simple internal coordinates: the $\text{H}-\text{O}_1$ bond, the $\text{C}-\text{O}_1$ bond, the $\text{C}-\text{O}_2$ bond, and the $\text{H}-\text{O}_1-\text{C}$ bond angle. LINX, in this case, is defined from a local Cartesian representation where the O_1-C bond length defines the y axis, and the H atom lies in the xy plane in the positively increasing x direction. LINX is actually the x component of the vector defined by the $\text{C}-\text{O}_2$ bond. Figure 1 displays a visual representation of this coordinate. LINY is defined from this same coordinate system, but it is the z component of the vector defined by the $\text{C}-\text{O}_2$ bond. LINY is zero in this case, as HOCO^+ is planar in its ground state.

The fundamental vibrational frequencies computed from both the CcCR and CR QFFs with both VPT and VCI are listed in Table IV along with the experimental data for both the gas and condensed phases as well as the DOCO^+ data discussed in Sec. III B. The VCI results given for both QFFs

are based on the 5-mode representation (5MR) of the anharmonic potential in Eq. (2) of Ref. 58. The 4MR VCI results agree with their 5MR counterparts to within 0.2 cm^{-1} indicating convergence of the mode coupling in the potential terms. Additionally, the VCI computations require 11 868 a' and 7251 a'' vibrational variational basis functions. Larger numbers of basis functions for specific modes are also employed to test for convergence, and the fundamental vibrational frequencies were affected by less than 0.4 cm^{-1} giving a clear statement of convergence. The VCI computations require 31 primitive functions. These are contracted down to 16 actual basis functions required for ν_1 and 14 actual bases for all other modes. Between 16 and 22 Gauss-Hermite quadrature points are necessary for the description of the six modes. The input for the VPT computations calls for explicit inclusion of two three-fold Fermi resonance polyads³⁵ for $\nu_2 = 2\nu_3 = \nu_3 + \nu_4$ and $\nu_3 = 2\nu_5 = 2\nu_6$ with the addition of a type-2 Fermi resonance for $\nu_1 = \nu_2 + \nu_4$, as well as a ν_5 and ν_6 Coriolis resonance.

TABLE IV. The CcCR and CR QFF fundamental vibrational frequencies (in cm^{-1}) for HOCO^+ and DOCO^+ from VPT and VCI computations as well as reported experimental results.

Mode	Description	CcCR		CR		Experiment		
		VPT	VCI	VPT	VCI	Condensed ^a	Gas phase ^b	
HOCO^+	ν_1	a' O_1-H stretch	3376.3	3376.2	3371.2	3374.8	3280.9	3375.374 13
	ν_2	a' $\text{C}-\text{O}_2$ stretch	2405.4	2407.6	2388.5	2395.0	2400.4	
	ν_3	a' $\text{C}-\text{O}_1$ stretch	1231.2	1223.9	1225.3	1224.3	...	
	ν_4	a' $\text{H}-\text{O}_1-\text{C}$ bend	1024.0	1022.2	1025.5	1028.6	1019.9	
	ν_5	a' $\text{O}_1-\text{C}-\text{O}_2$ bend	558.5	558.5	555.4	560.5	...	
	ν_6	a'' torsional mode	614.4	614.9	610.7	616.9	...	
	ZPE		4700.8	4679.8	4688.9	4675.5		
DOCO^+	ν_1	a' O_1-D stretch	2504.1	2510.8	2501.0	2520.2	2564.7	
	ν_2	a' $\text{C}-\text{O}_2$ stretch	2377.5	2381.0	2362.3	2353.2	2374.0	
	ν_3	a' $\text{C}-\text{O}_1$ stretch	1241.8	1239.7	1237.2	1238.9	...	
	ν_4	a' $\text{D}-\text{O}_1-\text{C}$ bend	845.2	844.3	845.8	849.4	843.0	
	ν_5	a' $\text{O}_1-\text{C}-\text{O}_2$ bend	497.1	496.3	495.2	498.7	...	
	ν_6	a'' torsional mode	596.9	596.8	593.4	599.0	...	
	ZPE		4087.0	4075.5	4076.2	4070.6		

^aNe matrix data from Ref. 31.

^bReference 28.

The first thing to note from Table IV is the good agreement between the frequencies computed with VPT and those computed with the VCI method. Regardless of the choice of QFF, the VPT fundamental frequencies are never more than 8 cm^{-1} larger or smaller than the corresponding VCI values. In fact, besides the CcCR ν_3 C–O₁ stretch and the CR ν_2 C–O₂ stretch and the ν_6 torsional mode frequencies, VCI and VPT report frequencies that are within 3 cm^{-1} of one another regardless of which QFF is scrutinized. Even though VPT for the CR QFF predicts ν_6 at 610.7 cm^{-1} while VCI predicts ν_6 at 616.9 cm^{-1} (a difference of 6.2 cm^{-1}), the difference between VPT and VCI for this same mode with the CcCR QFF is only 0.5 cm^{-1} with VCI again predicting the slightly larger frequency. Previously,^{32,33} VCI and VPT differed substantially (up to as much as 30 cm^{-1}) in their description of the torsional mode, but here the two methods are predicting values that are much more coincident with one another. As mentioned previously, HOCO⁺ differs noticeably in its molecular geometry than the related neutral radical or anionic species which requires the use of the LINX/LINY coordinates. Their inclusion appears to rectify the difference between VPT and VCI predicted for the torsional mode in the previous studies on the radicals and the anion.^{32,33} This coordinate system was, in fact, tested for the *trans*-HOCO radical, but its 126.949° O₁–C–O₂ bond angle was not close enough to linearity for this coordinate system to make any substantial effect on the agreement between VCI and VPT for the ν_6 fundamental.

There is the notable consistency in the prediction of the fundamental vibrational frequencies between the two QFFs as shown in Table IV. For VPT, the average difference between the use of the CcCR QFF and the CR QFF is 6.0 cm^{-1} with the ν_2 C–O₂ stretch being the outlier showing a difference in the QFFs of 16.9 cm^{-1} . VCI has a better average agreement between the QFFs at 4.1 cm^{-1} , but ν_2 again is responsible for the increase in this average as the difference between the QFFs for this mode with VCI is 12.6 cm^{-1} . In both cases the CcCR QFF predicts a higher frequency for ν_2 . Without the inclusion of the ν_2 frequency differences, the average agreement between the QFFs is much closer at 3.9 cm^{-1} for VPT and 2.5 cm^{-1} for VCI. Hence, the exclusion of the core correlation terms in the CR QFF does affect the prediction of the gas phase frequencies, but this is not a large effect here.

Comparison of our predicted fundamental vibrational frequencies to experimental results is also striking. For the known gas phase ν_1 fundamental vibrational frequency of HOCO⁺ at 3375.374 cm^{-1} from Amano and Tanaka,^{27,28} VCI predicts this frequency at 3376.2 cm^{-1} for the CcCR QFF and 3374.8 cm^{-1} for the CR QFF. Interestingly, our predictions bookend the actual experimental frequency with the CcCR prediction coming in a little high and the CR prediction coming in a little low. Regardless, both QFFs place the VCI ν_1 O₁–H stretch within less than 1 cm^{-1} of the gas phase experimental fundamental vibrational frequency. Previously, these same techniques were able to predict the O₁–H stretching frequency to within 3 cm^{-1} of experiment for the *trans*-HOCO radical.³² Now we are exhibiting spectroscopic accuracy in the prediction of this fundamental frequency.

Comparing the condensed phase frequencies to our theoretical results is a bit less clear since the effects of the matrix on the fundamental frequencies as compared to the actual gas phase results is rarely straightforward. Again, it was noted by Jacox and Thompson that a $\sim 120\text{ cm}^{-1}$ redshift from the gas phase is present in the condensed phase ν_1 frequency. It could be assumed that the other two observed condensed phase frequencies would exhibit similar shifts. However, for the two known gas phase fundamental vibrational frequencies of the *trans*-HOCO radical, comparison to frequencies of this molecule taken again in a neon matrix by Jacox and co-workers⁵⁹ results in only a 7.7 cm^{-1} redshift for ν_1 from gas phase data reported in Ref. 60 and a 4.6 cm^{-1} redshift for ν_2 .⁶¹ Neither of these are large shifts. The 120 cm^{-1} shift in ν_1 for the cation is substantially larger indicating a fundamental change in the geometry and/or chemical behavior of the neon matrix with the inclusion of the positively charged system.

In all three cases pertaining to HOCO⁺ and the *trans*-HOCO radical where gas phase and neon matrix frequencies are both known, the matrix isolation frequencies are lower in energy than the corresponding gas phase frequencies. Additionally, our fundamental vibrational frequencies for all three stretching modes of the *trans*-HOCO radical are predicted to lie within 8 cm^{-1} or less of their condensed phase counterparts.³² In light of this and even though we cannot conclusively determine the effects of the matrix on the frequencies, comparison of the condensed phase frequencies to their theoretical gas phase counterparts is useful, at the very least, to make sure these other modes are not grossly in error. The VCI ν_2 and ν_4 frequencies lie within 9 cm^{-1} of the condensed phase results. The ν_2 mode is again bookended by the CcCR and CR results, while both QFFs predict the condensed phase frequency of ν_4 at 1019.9 cm^{-1} to be lower in energy than the gas phase frequency. The consistency between predictions of gas phase and experimental condensed phase frequencies of the radical and the cation serves to bolster our prediction of highly accurate gas phase fundamental vibrational frequencies.

The last interesting note about our predicted gas phase fundamental vibrational frequencies of HOCO⁺ again deals with the ν_5 O₁–C–O₂ bend and the ν_6 torsional mode. Examination of the harmonic frequencies given in Table I and the anharmonic frequencies in Table IV displays a positive anharmonicity present for ν_5 and ν_6 . Previously, it was mentioned that agreement was very good between these individual modes with regards to the choice of QFF or, especially, the choice of vibrational analysis method. For the latter point, VPT and VCI for the CcCR QFF predict the same frequencies for ν_5 at 558.5 cm^{-1} and differ by only 0.5 cm^{-1} for ν_6 . (VPT is 614.4 cm^{-1} ; VCI is 614.9 cm^{-1} .) These frequencies are in line with those for the same modes in the radicals and the anion,^{32,33} but none of those systems exhibited a positive anharmonicity. None are pseudo-linear, either. Even so, the CcCR positive anharmonicity is slightly less than 23 cm^{-1} for ν_5 and 21 cm^{-1} for ν_6 . The use of pseudo-linear coordinates for *trans*-HOCO⁺ should not result in erroneous predictions of the fundamental frequencies. Most likely, this anharmonicity is a result of the linearity in the molecule where the harmonic computations give an erroneous initial guess and where

the anharmonic computations have the best chance of predicting physical reality. An indication of this behavior in the harmonic computations is shown in Table I where our harmonic vibrational frequencies for the O_1-C-O_2 bend and torsional mode computed from a highly accurate ground state geometry and a more descriptive potential and QFF are more than 25 cm^{-1} higher in energy than those computed previously by Francisco.³⁰

The consistency of the positive anharmonicity prediction for ν_5 and ν_6 between methods and QFFs also gives a solid indication that this is a real effect. The VCI potential is constructed from coupling the mode potentials, and the vibrational wavefunction employs linear combinations of harmonic functions for all the modes. Hence, it has the best chance to fully describe the system. However, VPT is predicting the ν_5 and ν_6 fundamental frequencies to be within 0.5 cm^{-1} of the VCI frequencies for the CcCR QFF even though the VPT procedure is different from that done in VCI. The corroboration in values between the two methods leads us to conclude that the positive anharmonicity is not a product of method choice. Although this result is unexpected, it is not outside of the realm of possibility since the use of QFFs conjoined to accurate vibrational analyses are designed to produce the most physically meaningful, even if surprising, results possible. Hence, the actual gas phase fundamental ν_5 and ν_6 frequencies of $HOCO^+$ should exhibit a positive anharmonicity.

B. $DOCO^+$

Deuterating the $HOCO^+$ cation to give $DOCO^+$ does not alter the equilibrium geometry, the force constants computed, or any values based solely on the electronic structure computations since the Born-Oppenheimer approximation is employed in these computations. However, Table II is different from Table I as the increased mass of the hydrogen affects $DOCO^+$ save for the equilibrium geometry. The zero-point rotational constants similarly compare with experiment as $HOCO^+$ does. B_0 and C_0 are again within 0.001 cm^{-1} of Bogey and co-workers' experiment²⁹ with the $DOCO^+$ A_0 values slightly better than $HOCO^+$ since agreement is now less than 0.07 cm^{-1} here. As expected the harmonic vibrational frequencies shift substantially, especially for those modes where the H or D atom is a major contributor to its motion. The $H/D-O_1$ stretch is affected the most as it decreases nearly 1000 cm^{-1} from 3561 cm^{-1} to 2603.1 cm^{-1} upon deuteration. Interestingly, the harmonic O_1-C-O_2 bending mode decreases by 44.1 cm^{-1} , while the torsional mode only decreases by 3.2 cm^{-1} .

The MULTIMODE computations utilize the same number of basis functions and computational details for $DOCO^+$ as they do for $HOCO^+$. The SPECTRO computations require input of the same Coriolis resonance as $HOCO^+$, but the three-fold Fermi resonance polyads are different with the need for inclusion of $\nu_1 = \nu_2 = 2\nu_3$ and $\nu_3 = 2\nu_5 = \nu_4 + \nu_6$. Table II also lists the rovibrational interaction and centrifugal distortion constants. Our theoretically computed rotational constants from Table II display even better agreement with the corresponding experimental data obtained by Bogey and co-

workers²⁹ for the $DOCO^+$ values relative to $HOCO^+$. This is certainly true of the D_J , D_{JK} , d_1 , and d_2 values where, for example, D_{JK} of $DOCO^+$ differs by less than 0.02 MHz between the work done in this study and that from experiment, while this difference is around 0.09 MHz for $HOCO^+$. Additionally, D_K is within 60 MHz of experiment, much closer than 400 MHz for $HOCO^+$, where some uncertainty in the $DOCO^+$ experiment is also mentioned by Bogey and co-workers.²⁹ Additionally, H_{KJ} is experimentally reported to be -364.4 Hz , while our computations put this value at -249.891 Hz .

Similar behavior is again predicted for the fundamental vibrational frequencies of this isotopologue as found for $HOCO^+$. Table IV reports the VPT and VCI CcCR and CR fundamental vibrational frequencies and the Ne matrix condensed phase data for $HOCO^+$ but also for $DOCO^+$ again from Jacox and Thompson.³¹ Correlation between methods for either QFF is strong. For the CcCR QFF, the VPT gives frequencies for ν_4 , ν_5 , and ν_6 that are within 1 cm^{-1} of VCI with the VPT ν_3 frequency within 2 cm^{-1} of VCI. The ν_1 and ν_2 frequencies have VPT and VCI values within 7 cm^{-1} . The agreement for the CR QFF is not as good, especially for ν_1 which VPT reports at 2501.0 cm^{-1} and VCI reports at 2520.2 cm^{-1} . Even so, besides ν_2 which differs by 9.1 cm^{-1} , the other modes do not differ in their frequencies between the methods by more than 5.6 cm^{-1} .

The agreement between methods with or without inclusion of core correlation effects in the QFF for $DOCO^+$ is also noteworthy. The one exception to this is the $\nu_2\text{ C}-O_2$ stretching mode as it is for $HOCO^+$. For VPT, the CcCR QFF reports this frequency at 2377.5 cm^{-1} while it is 2362.3 cm^{-1} for the CR QFF, a difference of 15.2 cm^{-1} . For VCI, this difference is even greater at 27.8 cm^{-1} since the CcCR QFF puts this frequency at 2381.0 cm^{-1} and the CR QFF at 2353.2 cm^{-1} . The next greatest difference between QFFs is 9.4 cm^{-1} for the VCI ν_1 mode. Even so, the average difference between QFFs for VPT is 4.8 cm^{-1} and 7.9 cm^{-1} for VCI. Removal of the ν_2 mode decreases the average difference to 2.7 cm^{-1} and 4.0 cm^{-1} , respectively. All of these results are reminiscent of $HOCO^+$ with the exception that the average difference between QFFs for a given method is greater with VCI for $DOCO^+$ where it is VPT that had the greater average difference for $HOCO^+$.

Comparison to the condensed phase experiments is also similar to $HOCO^+$. The ν_1 frequency is as much as 63.7 cm^{-1} higher and as little as 44.5 cm^{-1} higher than our results, specifically for CR VPT and VCI, respectively, in this example. This illustrates that the $H/D-O_1$ stretch is predicted by our methods to behave similarly but not to the same extent for $DOCO^+$ as it does for what is experimentally known and corroborated by our results for $HOCO^+$. The ν_2 mode frequency is once more bookended between the CcCR and CR QFFs for VCI with the 2381.0 cm^{-1} CcCR VCI frequency closer to the condensed phase result at 2374.0 cm^{-1} than the 2353.2 cm^{-1} CR VCI frequency. The ν_4 condensed phase frequency is reported to be 843.0 cm^{-1} , 1.3 cm^{-1} below the CcCR VCI frequency for this mode and 6.4 cm^{-1} below CR VCI. According to these computations, the condensed phase frequencies for ν_2 and ν_4 are again good approximations to

their gas phase counterparts for DOCO^+ , while the ν_1 condensed phase frequency is not as accurate for describing the gas phase behavior of this most energetic mode.

Lastly, there are positive anharmonicities present in the DOCO^+ vibrational computations, as well. The ν_5 and ν_6 modes again exhibit positive anharmonicities for this isotopologue, but the ν_3 C–O₁ stretch is also positively anharmonic. The positive anharmonicity for the DOCO^+ ν_3 frequency is 9.6 cm^{-1} computed with CcCR VCI at 1239.7 cm^{-1} . The positive anharmonicity for ν_6 is not as great for DOCO^+ as it is for its hydrogenated counterpart since the CcCR VCI frequency is 596.8 cm^{-1} , exactly 10.0 cm^{-1} higher than the harmonic. The ν_5 positive anharmonicity is 4.8 cm^{-1} for CcCR VCI. These are substantially smaller than the more than 20 cm^{-1} positive anharmonicity exhibited for HOCO^+ . The presence of an additional positive anharmonicity present in the post-harmonic vibrational analyses for DOCO^+ gives more indication that the harmonic vibrational frequencies struggle to adequately describe the fundamental vibrational frequencies of the H/DOCO^+ system and highlight even more reason to go beyond the harmonic approximation for the analysis of fundamental vibrational frequencies.

IV. CONCLUSIONS

As the use of infrared telescopes has grown, the need for more data in this range of electromagnetic spectrum for molecules known to exist in the ISM has also grown. Since protonated carbon dioxide or HOCO^+ is known to exist in the ISM from its rotational spectrum, cataloguing its fundamental vibrational frequencies is beneficial to the process of studying the heavens in the IR. Also, in the studies of $\text{OH} + \text{CO}$, HOCO^+ is a useful starting species in probing certain portions of the potential surface. Its fundamentals cannot be adequately approximated from harmonic computations, and experimental work is incomplete for the analysis of HOCO^+ and DOCO^+ . Only the O₁–H ν_1 stretching mode has been clearly experimentally observed and recorded $3375.37413\text{ cm}^{-1}$.^{27,28} Utilizing quartic force fields with vibrational perturbation theory and vibrational configuration interaction computations previously employed on closely related molecular species,^{32,33} we have been able to predict the gas phase ν_1 frequency of HOCO^+ to within 1 cm^{-1} accuracy. Since the agreement between the choice of QFFs and vibrational methods is quite good, we conclude that we are making reliable predictions of the other fundamental vibrational frequencies for this cation and its isotopologue DOCO^+ . Even though a positive anharmonicity is present in the computations of the ν_5 and ν_6 modes of both systems and the DOCO^+ ν_3 mode, the consistency of the computations to predict this behavior leads us to conclude that this is physically meaningful.

Additionally, reported experimental spectroscopic constants and geometrical parameters of both systems are in line with what is computed as part of this study. Our electronic structure computations also give a clear indication that a *cis* isomer of HOCO^+ does not exist. In all, we are providing an accurate prediction of the gas phase fundamental anharmonic vibrational frequencies and spectroscopic constants of

HOCO^+ in its stable *trans* conformation as well as the same data for the deuterated DOCO^+ system. This information may be of assistance in explaining phenomena related to interstellar studies, the $\text{OH} + \text{CO}$ potential surface, or other chemical circumstances.

ACKNOWLEDGMENTS

The U.S. National Science Foundation supported the work exhibited here by R.C.F. and T.D.C. through a Multi-User Chemistry Research Instrumentation and Facility (CRIF:MU) Award No. CHE-0741927 and through Award No. CHE-1058420. NASA Grant No. 10-APRA10-0096 and NASA Grant No. 08-APRA08-0050 supported the work undertaken by T.J.L. X.H. also acknowledges support from the NASA/SETI Institute Cooperative Agreement NNX09AI49A. The ChemVP program created by Dr. Andrew Simmonett of the University of Georgia was integral in the creation of Fig. 1. The authors are grateful for his allowance of our use of this program.

- ¹S. Green, H. Schor, P. Siegbahn, and P. Thaddeus, *Chem. Phys.* **17**, 479 (1976).
- ²E. Herbst, S. Green, P. Thaddeus, and W. Klemperer, *Astrophys. J.* **215**, 503 (1977).
- ³P. Thaddeus, M. Guélin, and R. A. Linke, *Astrophys. J.* **246**, L41 (1981).
- ⁴M. Bogey, C. Demuynck, and J. L. Destombes, *Astron. Astrophys.* **138**, L11 (1984).
- ⁵Y. C. Minh, W. M. Irvine, and L. M. Ziurys, *Astrophys. J.* **334**, 175 (1988).
- ⁶G. Pineau des Forêts, E. Roueff, and D. R. Flower, *J. Chem. Soc., Faraday Trans.* **85**, 1665 (1989).
- ⁷Y. C. Minh, M. K. Brewer, W. M. Irvine, P. Friberg, and L. E. B. Johansson, *Astron. Astrophys.* **244**, 470 (1991).
- ⁸S. Deguchi, A. Miyazaki, and Y. C. Minh, *Publ. Astron. Soc. Jpn.* **58**, 979 (2006).
- ⁹N. Sakai, T. Sakai, Y. Aikawa, and S. Yamamoto, *Astrophys. J.* **675**, L89 (2008).
- ¹⁰S. Petrie, *Mon. Not. R. Astron. Soc.* **251**, 468 (1991).
- ¹¹M. Aschi and A. Largo, *Int. J. Mass Spectrom.* **228**, 613 (2003).
- ¹²K. Hamammi, F. Lique, N. Jaïdane, Z. Ben Lakhdar, A. Spielfiedel, and N. Feautrier, *Astron. Astrophys.* **462**, 789 (2007).
- ¹³N. S. Shuman, W. R. Stevens, and T. Baer, *Int. J. Mass Spectrom.* **294**, 88 (2010).
- ¹⁴N. S. Shuman, M. Johnson, W. R. Stevens, M. E. Harding, J. F. Stanton, and T. Baer, *J. Chem. Phys.* **A 114**, 10016 (2010).
- ¹⁵L. Paetow, F. Unger, W. Beichel, G. Frenking, and K.-M. Weitzel, *J. Chem. Phys.* **132**, 174305 (2010).
- ¹⁶L. Paetow, F. Unger, B. Beutel, and K.-M. Weitzel, *J. Chem. Phys.* **133**, 234301 (2010).
- ¹⁷D. E. Woon, *Astrophys. J.* **728**, 44 (2011).
- ¹⁸D. Troya, M. J. Lakin, G. C. Schatz, and L. B. Harding, *J. Phys. Chem. B* **106**, 8148 (2002).
- ¹⁹M. J. Lakin, D. Troya, G. C. Schatz, and L. B. Harding, *J. Chem. Phys.* **119**, 5848 (2003).
- ²⁰J. D. Savee, J. E. Mann, and R. E. Continetti, *J. Chem. Phys.* **A 114**, 1485 (2010).
- ²¹J. S. Francisco, J. T. Muckerman, and H.-G. Yu, *Acc. Chem. Res.* **43**, 1519 (2010).
- ²²J. Li, Y. Wang, B. Jiang, J. Ma, R. Dawes, D. Xie, J. M. Bowman, and H. Guo, *J. Chem. Phys.* **136**, 041103 (2012).
- ²³U. Seeger, R. Seeger, J. A. Pople, and P. v. R. Schleyer, *Chem. Phys. Lett.* **55**, 399 (1978).
- ²⁴D. J. DeFrees, G. H. Loew, and A. D. McLean, *Astrophys. J.* **254**, 405 (1982).
- ²⁵P. R. Taylor and M. Scarlett, *Astrophys. J.* **293**, L49 (1985).
- ²⁶M. J. Frisch, H. F. Schaefer III, and J. S. Binkley, *J. Phys. Chem.* **89**, 2192 (1985).

- ²⁷T. Amano and K. Tanaka, *J. Chem. Phys.* **82**, 1045 (1985).
- ²⁸T. Amano and K. Tanaka, *J. Chem. Phys.* **83**, 3721 (1985).
- ²⁹M. Bogey, C. Demuyne, J. L. Destombes, and A. Krupnov, *J. Mol. Struct.* **190**, 465 (1988).
- ³⁰J. S. Francisco, *J. Chem. Phys.* **107**, 9039 (1997).
- ³¹M. E. Jacox and W. E. Thompson, *J. Chem. Phys.* **119**, 10824 (2003).
- ³²R. C. Fortenberry, X. Huang, J. S. Francisco, T. D. Crawford, and T. J. Lee, *J. Chem. Phys.* **135**, 134301 (2011).
- ³³R. C. Fortenberry, X. Huang, J. S. Francisco, T. D. Crawford, and T. J. Lee, *J. Chem. Phys.* **135**, 214303 (2011).
- ³⁴T. J. Lee, J. M. L. Martin, and P. R. Taylor, *J. Chem. Phys.* **102**, 254 (1995).
- ³⁵J. M. L. Martin, T. J. Lee, P. R. Taylor, and J.-P. François, *J. Chem. Phys.* **103**, 2589 (1995).
- ³⁶X. Huang and T. J. Lee, *J. Chem. Phys.* **129**, 044312 (2008).
- ³⁷X. Huang and T. J. Lee, *J. Chem. Phys.* **131**, 104301 (2009).
- ³⁸X. Huang, P. R. Taylor, and T. J. Lee, *J. Phys. Chem. A* **115**, 5005 (2011).
- ³⁹K. Raghavachari, G. W. Trucks, J. A. Pople, and M. Head-Gordon, *Chem. Phys. Lett.* **157**, 479 (1989).
- ⁴⁰A. P. Rendell, T. J. Lee, and P. R. Taylor, *J. Chem. Phys.* **92**, 7050 (1990).
- ⁴¹J. M. L. Martin and T. J. Lee, *Chem. Phys. Lett.* **200**, 502 (1992).
- ⁴²C. E. Dateo, T. J. Lee, and D. W. Schwenke, *J. Chem. Phys.* **101**, 5853 (1994).
- ⁴³A. C. Scheiner, G. E. Scuseria, J. E. Rice, T. J. Lee, and H. F. Schaefer III, *J. Chem. Phys.* **87**, 5361 (1987).
- ⁴⁴G. E. Scuseria, *J. Chem. Phys.* **94**, 442 (1991).
- ⁴⁵T. H. Dunning, *J. Chem. Phys.* **90**, 1007 (1989).
- ⁴⁶K. A. Peterson and T. H. Dunning, *J. Chem. Phys.* **102**, 2032 (1995).
- ⁴⁷R. A. Kendall, T. H. Dunning, and R. J. Harrison, *J. Chem. Phys.* **96**, 6796 (1992).
- ⁴⁸J. M. L. Martin and P. R. Taylor, *Chem. Phys. Lett.* **225**, 473 (1994).
- ⁴⁹INTDER 2005 is a general program written by W. D. Allen and co-workers, which performs vibrational analysis and higher order nonlinear transformations, 2005.
- ⁵⁰J. M. L. Martin and T. J. Lee, *Chem. Phys. Lett.* **258**, 136 (1996).
- ⁵¹M. Douglas and N. Kroll, *Ann. Phys.* **82**, 89 (1974).
- ⁵²H.-J. Werner, P. J. Knowles, F. R. Manby, M. Schütz *et al.*, MOLPRO, version 2010.1, a package of *ab initio* programs, 2010, see <http://www.molpro.net>.
- ⁵³J. F. Gaw, A. Willets, W. H. Green, and N. C. Handy, SPECTRO program, version 3.0, 1996.
- ⁵⁴I. M. Mills, in *Molecular Spectroscopy – Modern Research*, edited by K. N. Rao and C. W. Mathews (Academic, New York, 1972).
- ⁵⁵J. K. G. Watson, in *Vibrational Spectra and Structure*, edited by J. R. Durig (Elsevier, Amsterdam, 1977).
- ⁵⁶D. Papousek and M. R. Aliev, *Molecular Vibration-Rotation Spectra* (Elsevier, Amsterdam, 1982).
- ⁵⁷S. Carter, J. M. Bowman, and N. C. Handy, *Theor. Chem. Acc.* **100**, 191 (1998).
- ⁵⁸J. M. Bowman, S. Carter, and X. Huang, *Int. Rev. Phys. Chem.* **22**, 533 (2003).
- ⁵⁹D. Forney, M. E. Jacox, and W. E. Thompson, *J. Chem. Phys.* **119**, 10814 (2003).
- ⁶⁰J. T. Petty and C. B. Moore, *J. Mol. Spectrosc.* **161**, 149 (1993).
- ⁶¹T. J. Sears, W. M. Fawzy, and P. M. Johnson, *J. Chem. Phys.* **97**, 3996 (1992).